Optics Letters

Single-frequency CW Ti:sapphire laser with intensity noise manipulation and continuous frequency-tuning

Pixian Jin,[1] Huadong Lu,[1,2,*] Yixiao Wei,[1] Jing Su,[1,2] and Kunchi Peng[1,2]

[1]State Key Laboratory of Quantum Optics and Quantum Optics Devices, Institute of Opto-electronics, Shanxi University, Taiyuan, Shanxi 030006, China
[2]Collaborative Innovation Center of Extreme Optics, Shanxi University, Taiyuan, Shanxi 030006, China
*Corresponding author: luhuadong@sxu.edu.cn

Received 15 November 2016; revised 8 December 2016; accepted 9 December 2016; posted 9 December 2016 (Doc. ID 280943); published 23 December 2016

We present a tunable single-frequency CW Ti:sapphire laser with intensity noise manipulation. The manipulation of the laser intensity noise is realized by varying the frequency of the modulation signal loaded on the electrodes of an intracavity electro-optic etalon. A lithium niobate ($LiNbO_3$) crystal is used to act as the electro-optic etalon, and its electro-optic effect is utilized to modulate the intracavity laser intensity for locking itself to the oscillating wavelength of the laser to implement continuous frequency-tuning. When the electro-optic etalon is locked to the oscillating mode of the Ti:sapphire laser with arbitrarily selected modulation frequency, the maximal continuous frequency-tuning range can reach to 20 GHz, and the laser intensity noise is successfully manipulated simultaneously. © 2016 Optical Society of America

OCIS codes: (140.3590) Lasers, titanium; (140.3600) Lasers, tunable; (140.3570) Lasers, single-mode; (140.3560) Lasers, ring.

https://doi.org/10.1364/OL.42.000143

All-solid-state continuous-wave (CW) single-frequency tunable Ti:sapphire lasers can generate near-infrared light covering alkali atomic transition lines and have become significant resources in atom-based experimental research and applications, such as atom trapping and cooling [1], atomic clocks [2], quantum storage [3], optical magnetometry [4], atomic force microscopy, and so on. Especially, with the development of optical magnetometry, probing atomic spin ensembles with a polarization-squeezed beam at low frequency can effectively improve the sensitivity of a magnetometer [4]. The primary key of establishing a polarization-squeezed beam at low frequency is an available, stable single-frequency Ti:sapphire laser with continuous frequency-tuning and low intensity noise. Nowadays, four commercial types of continuous frequency-tuning Ti:sapphire laser developed by Coherent [5], Spectra-Physics [6], Tekhnoscan Joint-Stock [7], and M-square [8], respectively, are available to scientists and engineers. In order to realize the continuous frequency-tuning, a PZT-based etalon locking system is adopted in all of these lasers, where the frequency of the modulation signal is required to correspond to the resonant frequency of the PZT, generally in the kilohertz region, to obtain a well-defined error signal. The modulation signal increases the intensity noise of the laser at that frequency, which enhances the difficulty of the laser intensity noise reduction and polarization-squeezed beam establishment at low frequency range. For the purpose of reducing this difficulty, a continuously tunable single-frequency Ti:sapphire laser with intensity noise manipulation or suppression is desired. In 2014, our group obtained a continuous frequency-tuning Ti:sapphire laser by means of the additional intracavity nonlinear loss introduced by a nonlinear crystal [9]. The frequency scanning range of 48 GHz was realized, and the intensity noise of the laser at lower frequency was effectively suppressed. This method did not need the modulation locking system to lock the intracavity etalon. Nevertheless, the frequency scanning of the laser can only be limited within a special frequency range, which was decided by the phase-matching bandwidth of the nonlinear crystal for second-harmonic generation (SHG).

In this Letter, we present a CW single-frequency Ti:sapphire laser with continuous frequency-tuning, whose intensity noise can be freely manipulated. The continuous frequency-tuning is achieved by means of an intracavity locked electro-optic etalon, and the intensity noise is manipulated by choosing the frequency of the modulation signal loaded on the electrodes of the electro-optic etalon. The electro-optic etalon is acted by a lithium niobate ($LiNbO_3$) crystal owing to its high electro-optic coefficient. The maximal tuning range of 110 nm by rotating the birefringent filters (BRFs) and the continuous frequency-tuning range of 20 GHz after the electro-optic etalon is locked to the oscillating wavelength of the Ti:sapphire laser with arbitrarily selected modulation frequency are achieved, respectively. The intensity noise of the Ti:sapphire laser is also successfully manipulated by varying the frequency of the modulation signal.

The configuration of the designed all-solid-state CW single-frequency Ti:sapphire laser with continuous frequency-tuning

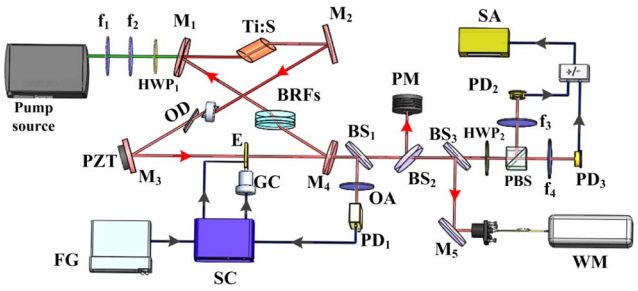


Fig. 1. Experimental setup of the continuous frequency-tuning laser. HWP_1 and HWP_2, half-wave-plate; Ti:S, Ti:sapphire; OD, optical diode; BRFs, birefringent filters; E, etalon; GC, galvanometer scanner; FG, function generator; SC, servo controller; OA, optical attenuator; PD_1-PD_3, photodetectors; BS_1-BS_3, beam splitter; PBS, polarization beam splitter; PM, power meter; WM, wavelength meter; SA, spectral analyzer.

and experimental setup are shown in Fig. 1. A bow-tie ring cavity is formed by two concave–convex mirrors with a curve radius of 100 mm (M_1 and M_2) and two plane mirrors (M_3 and M_4). M_1 and M_2 are both coated with high-reflection (HR) films at 740–890 nm and antireflection (AR) films at 532 nm. M_3 and M_4 are coated with HR film at 740–890 nm and partial transmission film at 740–890 nm ($T = 5.5\%$), respectively. In order to avoid the harmful influence of the parasitic absorption and realize the broadband tuning, a Brewster-angle-cut (60.4°) Ti:sapphire crystal with a doping concentration of 0.05 wt. % and size of Φ4 mm × 20 mm is adopted, which is mounted in a closed copper block oven cooled by circulated water and positioned between the curved mirrors M_1 and M_2. In order to obtain a stable and tunable single-frequency Ti:sapphire laser, a homemade all-solid-state CW single-frequency 532 nm laser with output power of 18 W and stability better than ±0.5% (8 h) [10] is used as the pump source [11] (DPSS FG-VIIIB, Yuguang Co., Ltd). The output beam of the pump source with the waist diameter of 160 μm is coupled into the resonator and is focused at the center of the Ti:sapphire crystal. The optical coupler is a telescope system consisting of the lenses f_1 and f_2 with focal lengths of 200 mm and 100 mm, respectively, which can form a waist diameter of 80 μm at the center of the Ti:sapphire crystal. The half-wave plate (HWP_1) in front of the resonator is used to align the polarization of the incident pump laser beam to satisfy the requirement of the Ti:sapphire crystal. The broad bandwidth optical diode (OD) consisting of a thin quartz plate and a terbium gallium garnet (TGG) crystal surrounded by a permanent magnet can ensure unidirectional operation of the laser. The three-plate BRFs with thickness of 1 mm, 2 mm, and 4 mm is served for coarse frequency selection and tuning element and inserted into the resonator with its Brewster incident angle (57°). An electro-optic etalon made of $LiNbO_3$ crystal adhered to the rotation axis of the galvanometer scanner (GC) is used to suppress the mode-hop and finely tune the oscillating frequency by adjusting its incident angle. Continuously scanning the cavity length of the Ti:sapphire laser is implemented by scanning the voltage of the PZT adhered to M_3. In order to compensate the astigmatism induced by Ti:sapphire crystal, OD, and BRFs and enhance the optical-to-optical conversion efficiency, the folding angles of mirrors M_1 and M_2 are set to 15.8° [12].

A fractional of the output beam separated by the beam splitter (BS_1) is used to lock the electro-optic etalon with a phase-lock system consisting of a photodetector (PD_1, S3399, Hamamatsu Corporation), function generator (FG, DG1022U, RIGOL Technologies, Inc.), and homemade servo controller (SC). Most of the laser leaked from BS_1 is reflected by BS_2 to a power meter (PM, LabMax-TOP, Coherent) to monitor and record the output power of the laser. The remaining laser beam transmitted from BS_2 is split into two parts by BS_3. The one part is coupled into a wavelength meter (WM, WS6/765, High Finesse Laser and Electronic System) to record the output wavelength; the other part is injected to the self-homodyne-detector with the common mode rejection ratio of 34 dB to measure the intensity noise of the laser. The self-homodyne-detector includes a pair of photodetectors (PD_2 and PD_3, S3399, Hamamatsu Corporation) and a positive/negative power combiner. The measured noise spectrum is analyzed by a spectral analyzer (SA) with a resolution bandwidth (RBW) of 30 kHz and a video bandwidth (VBW) of 30 Hz.

To implement the CW Ti:sapphire laser with continuous frequency tuning and intensity noise manipulation, the $LiNbO_3$ electro-optic etalon is chosen as the intracavity fine frequency selector and tuner. Its dimensions are 10 mm × 1 mm × 5 mm ($X \times Y \times Z$) with its optical axis along the z axis, as shown in Fig. 2. The transmission surface of the crystal is uncoated and polished. The incident laser beam propagates through the crystal as ordinary light. When a modulation signal $V \cos \omega t$ is applied to the crystal along its optical axis through the electrodes, the corresponding frequency shift of its transmission peak can be expressed as [13]

$$d\nu = \frac{c n_o^2 \gamma_{13} V}{2\lambda d} \cos \omega t, \tag{1}$$

where c is the speed of light in vacuum, n_o is the ordinary index of refraction of the crystal, γ_{13} is the electro-optic coefficient, V is the amplitude of the signal, λ is the wavelength of the incident laser beam, d is the distance between two electrodes, and ω is the angular frequency of the signal. The periodic shift of the transmission peak of the etalon leads to the intracavity laser intensity, which is modulated and used to lock the etalon. Owing to the electro-optic effect, the $LiNbO_3$ crystal is independent of the frequency of the applied electric field; thus the modulation frequency in the laser system can be chosen arbitrarily in theory. To avoid mode-hop in the modulating process, the frequency shift of the transmission peak of the etalon should be less than one free spectral range (FSR) of the laser resonator, c/L, where L is the length of the laser cavity. Thus, the maximal amplitude of the modulation signal applied to the etalon is given as

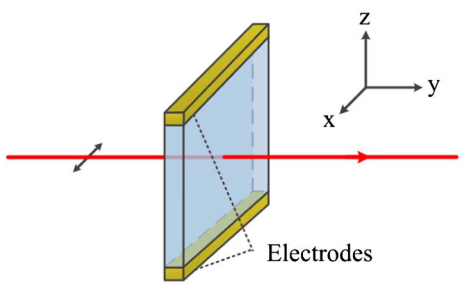


Fig. 2. Structure chart of the electro-optic etalon.

$$V_{\max} = \frac{2\lambda d}{L n_o^2 \gamma_{13}}. \quad (2)$$

According to the above analysis, the suitable amplitude of the modulation signal applied to the etalon should be carefully selected in the experiment.

When the Ti:sapphire laser was working at the wavelength of 795 nm, which corresponded to the D_1 line of Rubidium atoms, the output power versus the pump power were recorded, as shown in Fig. 3. The threshold pump power was 3.58 W, and the maximum output power of 2.88 W was obtained under the pump power of 16.53 W, where the slope efficiency was 22%. The inset of the Fig. 3 was the spatial beam profile of the output laser beam recorded by a beam quality meter (M2SETVIS, Thorlabs), and the measured values of M_x^2 and M_y^2 were 1.02 and 1.11, respectively. By rotating the BRFs and changing the included angle between the incident laser beam and the optical axis of BRFs, the oscillating wavelength can be tuned from 760 to 870 nm, and the obtained tuning range reached up to 110 nm. Tilting the electro-optical etalon can further fine-tune the oscillating frequency of the laser, and 58 GHz was achieved.

To realize continuous frequency-tuning of the Ti:sapphire laser, the transmission peak of the etalon had to be locked to the oscillating mode of the laser near the wavelength of 795 nm and could shift with the sliding of the oscillating mode of the laser. First, the performance of the electro-optic etalon was tested in experiment by applying a high-voltage dc signal varying from −1000 to 1000 V to the etalon and observing the variation of the laser output wavelength. The observed result is shown in Fig. 4. The one hop of the laser output wavelength corresponds to the frequency of the transmission peak of etalon shifting one FSR of the laser cavity. The result showed that the practical maximal modulation amplitude applied to the etalon should be 450 V. In experiments, the modulation amplitude of 250 V was applied, which was sufficient to generate the modulation of the intracavity laser intensity to be detected. From the result, it also can be found that the maximal tuning range of the oscillating frequency was 2.435 GHz by applying up to a 2000 V signal to the electro-optic etalon, which was narrower than the desired continuous frequency tuning range (larger than 20 GHz). Thus, the etalon was locked by slightly rotating its incident angle with drift of the oscillation mode of the laser. To generate the modulation, a modulation signal with an

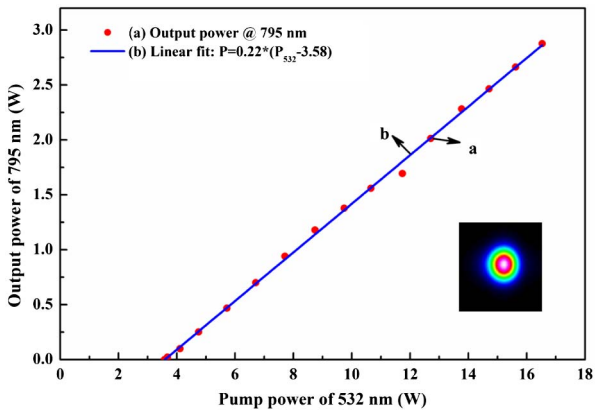


Fig. 3. Output power of Ti:sapphire laser at 795 nm versus the pump power. Inset: spatial beam profile of output laser.

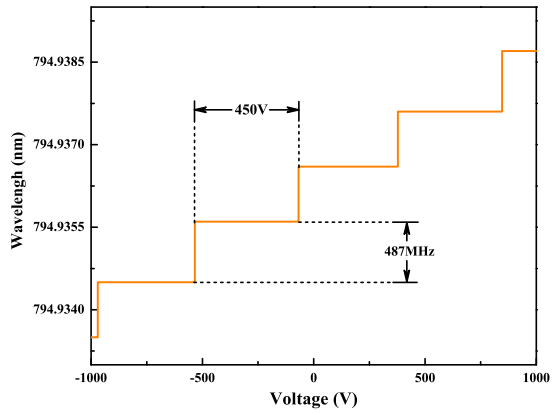


Fig. 4. Variation of the output wavelength of the Ti:sapphire laser with varied high-voltage dc signal applied to the etalon.

amplitude of 250 V, which was generated by FG and amplified by the high-voltage operational amplifier PA85 assembled in SC, as shown in Fig. 5, was applied to the etalon. A fraction of laser separated from the output beam by the BS_1 was detected by PD_1 with a bandwidth of higher than several million hertz. The PD_1 had sufficiently high gain, about 50 dB, for the ac-like part of the laser intensity is too small relative to the dc-like part. The detected signal was mixed with the modulation signal to extract the error signal in the SC. The generated error signal was amplified and integrated with the time constant of 8 ms to act on the GC to control the angle of the etalon. Manually adjusting the angle of the etalon and turning on the locking switch of the servo controller when the frequency of the detected signal was twice that of the modulation signal [14], the transmission peak of the etalon could be locked to the oscillation mode of the laser.

When the electro-optic etalon was locked to the oscillation wavelength of 795.0046 nm with the modulation frequency of 50 kHz, and a high-voltage scanning signal with amplitude and frequency of 400 V and 0.05 Hz, respectively, was applied to PZT to continuously scan the length of the laser cavity, the maximal frequency scanning range of 20 GHz was realized, as shown in Fig. 6(a). The nonlinear variation of the output wavelength with scanning time (or scanning voltage) resulted from the nonlinearity of the PZT. As previously mentioned, the selection of the modulation frequency was theoretically unlimited. To confirm this, six different modulation frequencies (32, 50, 84, 100, 123, and 150, respectively) were chosen arbitrarily in experiments, and the corresponding obtained continuous frequency tuning ranges were 21.5, 20, 22, 21, 21.5, and 20 GHz, which demonstrated that the modulation

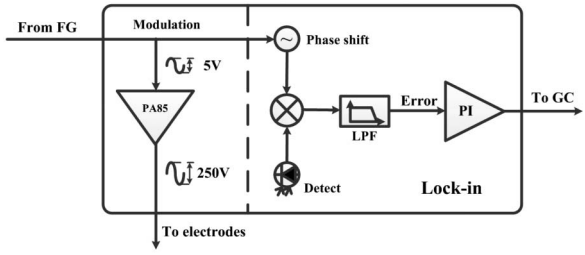


Fig. 5. Schematic of the servo controller.

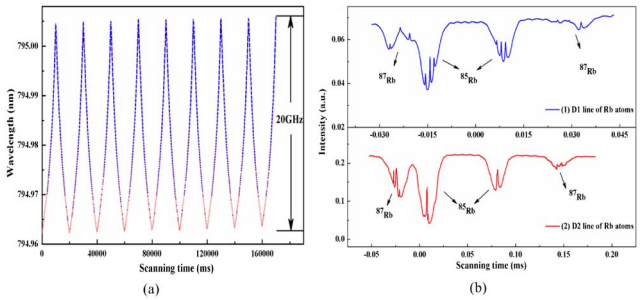


Fig. 6. (a) Continuously frequency tuning of the Ti:sapphire laser. (b) Saturation absorption spectroscopy of the Rb atoms. (1) D_1 line and (2) D_2 line.

frequency used in the process of etalon locking did not influence the property of continuous frequency-tuning of the Ti:sapphire laser. The obtained continuous frequency-tuning Ti:sapphire laser was used to scan the saturation absorption spectroscopy of the transition lines of rubidium atoms (^{85}Rb and ^{87}Rb). The transition curves were shown in Fig. 6(b). Curves 1 and 2 corresponded to D_1 and D_2 transition lines near the wavelengths of 795 and 780 nm, respectively.

In the case of realizing the continuous frequency-tuning after the intracavity electro-optical etalon was locked to the oscillating wavelength of the Ti:sapphire laser with different modulation frequencies, the intensity noise also could be successfully manipulated. It is well known that the modulation signal of the locking system heaves with a bump at modulation frequency in the intensity noise spectrum of the laser, which is harmful for the intensity noise reduction at this frequency. In order to eliminate the influence of the modulation signals on the intensity noise and expand the application of the presented Ti:sapphire laser, the frequency of the modulation signal loaded on the electrodes of the electro-optical etalon can be chosen beyond the interesting frequency range, which was the prominent advantage of the locked electro-optical etalon compared with the PZT-based etalon locking system. In the experiment, the intensity noises of the Ti:sapphire laser were measured with the modulation frequencies of 140, 180, and 220 kHz, respectively, which are depicted in Fig. 7. The peak of the laser intensity noise spectrum at modulation frequency was observed,

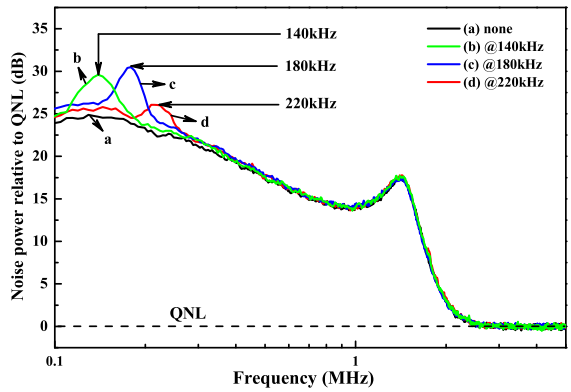


Fig. 7. Intensity noise of the Ti:sapphire laser at different modulation frequencies. (a) Without modulation signal, (b) at 140 kHz, (c) at 180 kHz, and (d) at 220 kHz.

and the position of the peak of the intensity noise spectra shifted with variation of the modulation frequency. The results showed that the intensity noise of the continuous frequency-tuning Ti:sapphire laser could be manipulated by changing the frequency of the modulation signal, which was significant for the suppression of the laser intensity noise at an interesting frequency range.

In conclusion, an all-solid-state CW single-frequency Ti:sapphire laser with continuous frequency-tuning and intensity noise manipulation has been achieved via intracavity-locked $LiNbO_3$ electro-optic etalon. The maximal tuning range of 110 nm (from 760 to 870 nm) was first achieved by rotating the BRFs. When the laser was working at the wavelength of 795 nm, the maximal output power of 2.88 W was obtained under the pump power of 16.53 W. The threshold pump power and the slope efficiency of the laser were 3.58 W and 22%, respectively. After the electro-optic etalon was locked to the oscillating mode of the Ti:sapphire laser with six sets of modulation signals with the same amplitudes of 250 V and different frequencies, which were arbitrarily selected, the continuous frequency-tuning ranges of 20 GHz were all realized. When the laser was working near the 780 and 795 nm, respectively, it was successfully utilized to scan the saturation absorption spectroscopy of the D_2 and D_1 transition lines of rubidium atoms. At last, the intensity noise of the obtained Ti:sapphire laser was successfully manipulated by varying the frequency of the modulation signal. The obtained all-solid-state CW signal-frequency Ti:sapphire laser with continuous frequency-tuning and intensity noise manipulation can be well used in the establishment of a polarization-squeezed beam at a low frequency range.

Funding. Key Project of the Ministry of Science and Technology of China (2016YFA0301401); National Natural Science Foundation of China (NSFC) (61227015, 61227902, 61405107); National Foundation Fund of Personnel Training (J1103210).

REFERENCES

1. T. Kuwamoto, K. Honda, Y. Takahashi, and T. Yabuzaki, Phys. Rev. A **60**, R745 (1999).
2. Z. W. Barber, C. W. Hoyt, C. W. Oates, and L. Hollberg, Phys. Rev. Lett. **96**, 083002 (2006).
3. Z. X. Xu, Y. L. Wu, L. Tian, L. R. Chen, Z. Y. Zhang, Z. H. Yan, S. J. Li, and H. Wang, Phys. Rev. Lett. **111**, 240503 (2013).
4. F. Wolfgram, A. Cerè, F. A. Beduini, A. Predojević, M. Koschorreck, and M. W. Mitchell, Phys. Rev. Lett. **105**, 053601 (2010).
5. http://www.coherent.com/Products/index.cfm?846/MBR-Ring-Series.
6. http://www.spectra-physics.com/products/tunable-lasers/matisse.
7. S. Kobtsev, V. Baraoulya, and V. Lunin, Proc. SPIE **6451**, 64511U (2007).
8. http://www.m2lasers.com/lasers/all-lasers/solstis-ti-sapphire-laser.aspx.
9. H. D. Lu, X. J. Sun, M. H. Wang, J. Su, and K. C. Peng, Opt. Express **22**, 24551 (2014).
10. Q. W. Yin, H. D. Lu, J. Su, and K. C. Peng, Opt. Lett. **41**, 2033 (2016).
11. H. D. Lu, J. Su, C. D. Xie, and K. C. Peng, Opt. Express **19**, 1344 (2011).
12. Y. Sun, H. D. Lu, and J. Su, Acta Sin. Quantum Opt. **14**, 344 (2008).
13. L. Cabaret, P. Camus, R. Leroux, and J. Philip, Opt. Lett. **26**, 983 (2001).
14. X. J. Sun, J. Wei, W. Z. Wang, and H. D. Lu, Chin. Opt. Lett. **13**, 071401 (2015).